Carbon monoxide during pollution events in Asia: Evolution and trends from 17 years of IASI data

Selviga Sinnathamby[1], S. Safieddine[1], C. Viatte C.[1], A. Boynard[1,2] , J. Hadji-Lazaro[1], M. George[1], D. Hurtmans[3], P. Coheur[3], M. Doutriaux-Boucher[4], J. Onderwaater[4] and C. Clerbaux[1,3]

[1]LATMOS/IPSL, Sorbonne Université, UVSQ, CNRS, Paris, France (selviga.sinnathamby@latmos.ipsl.fr)
[2]SPASCIA, Ramonville-Saint-Agne, 31520, France
[3]Spectroscopy, Quantum Chemistry and Atmospheric Remote Sensing (SQUARES), Université libre de Bruxelles (ULB), Brussels, Belgium
[4]EUMETSAT, Darmstadt, Germany

Introduction – Pollution events in Asia

- Asia has undergone rapid industrialization and demographic growth, leading to significant emissions of pollutants in recent years.
- Some regions in Asia frequently experience **severe air pollution events** (Northern India and Pakistan, November 2024).

Yibin, China
[Dheera Venkatraman & Wang Xi]

The New York Times | https://www.nytimes.com/2024/11/19/world/asia/india-delhi-air-pollution.html

Delhi Trudges Through Another Air Pollution Nightmare With No Answers

The government seems powerless to protect its citizens from this annual crisis, let alone prevent it.

India Gate in New Delhi was enveloped with smog on Tuesday. Anushree Fadnavis/Reuters

Introduction – IASI CO Climate Data Record

- Since 2007, IASI has been monitoring global and regional **carbon monoxide** (CO) concentrations, twice a day [Clerbaux et al., 2009].
- CO is mainly emitted during incomplete combustion processes (anthropogenic activities and biomass burning) and is eliminated by OH in late spring-summer.

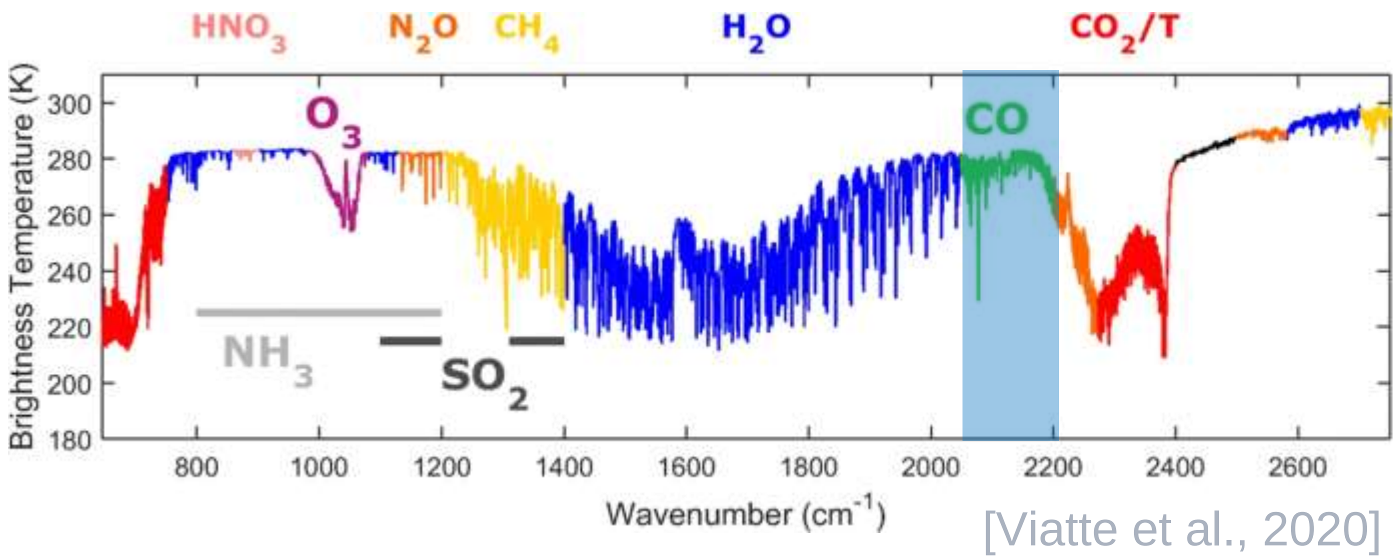

[Viatte et al., 2020]

- It is a good marker of pollution, with its lifetime of a few days to 2 months [Holloway et al., 2000].

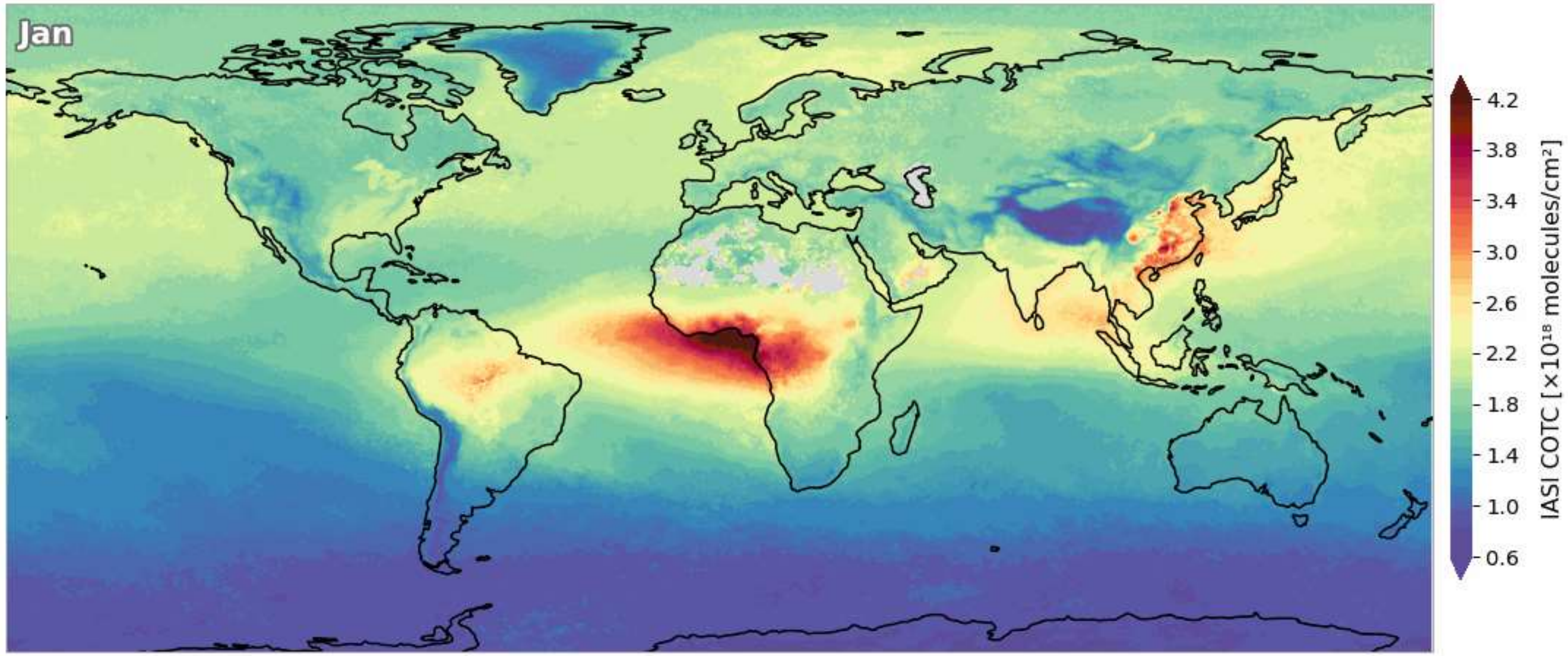

- For the first time, EUMETSAT reprocessed the IASI CO dataset (**Climate Data Record**, doi:10.15770/EUM_SAF_AC_0047), providing a homogeneous record of CO which allows us to do trends studies.

Introduction – Areas of study

- We will focus on CO total column (COTC) evolution and trends as seen by IASI over 2007-2024 in 3 areas :
  - North China Plain (**NCP**)
  - Mainland South-East Asia (**Mainland SEA**)
  - Indo-Gangetic Plain (**IGP**)

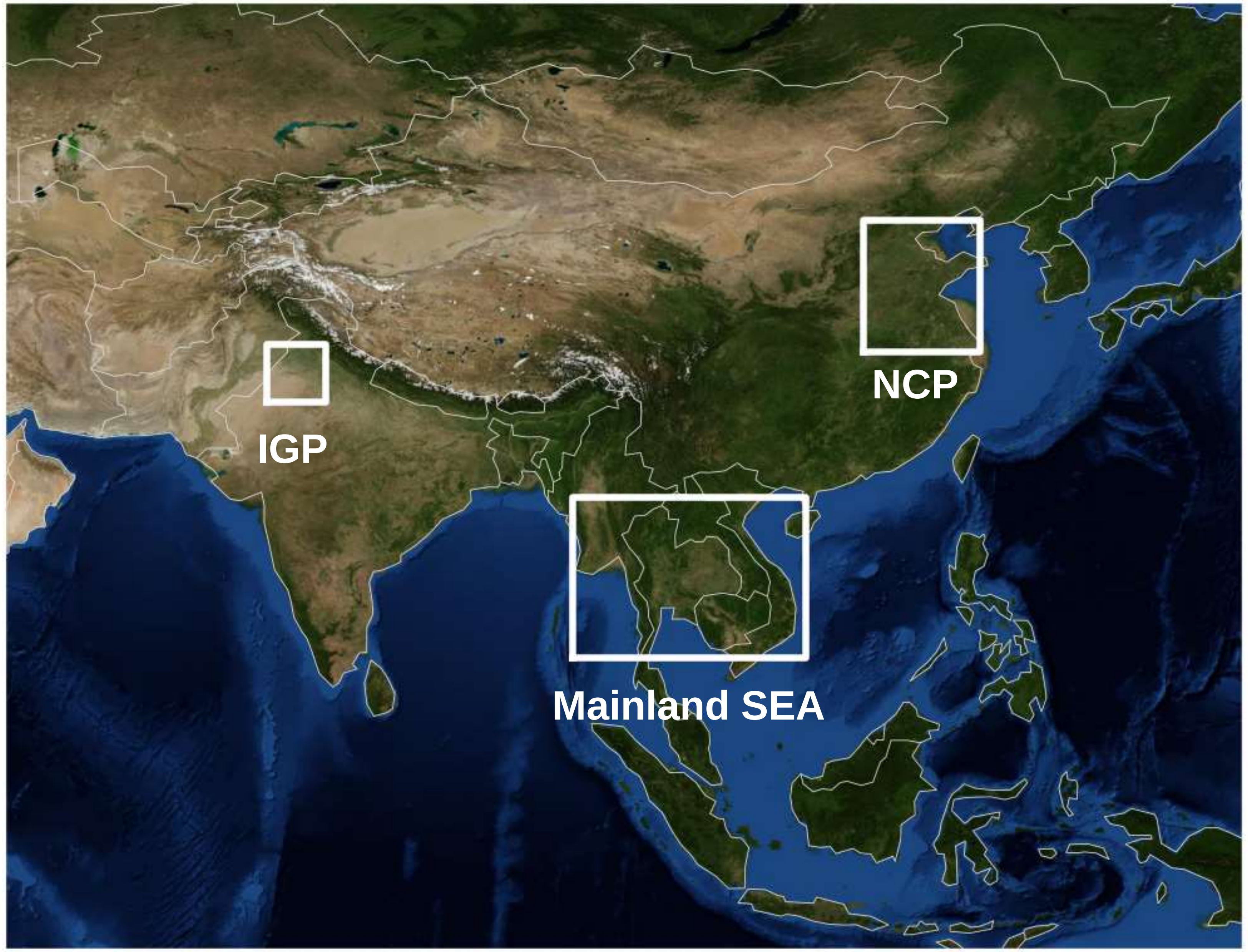

Methods – IASI's sensitivity and importance of nighttime data

- Thermal infrared instruments are known to be sensitive in the mid-troposphere [George et al., 2015].
- However, they can have a high sensitivity close to the surface in cases of **strong negative thermal contrast** (temperature difference between the surface and the atmospheric layer just above the surface) [Bauduin et al., 2017].

→ we need to include nighttime data.

- As high thermal contrast is associated with low COTC error, we apply a **error-based filter** on IASI daytime and nighttime data.

Example case : IGP, 2023/11/06

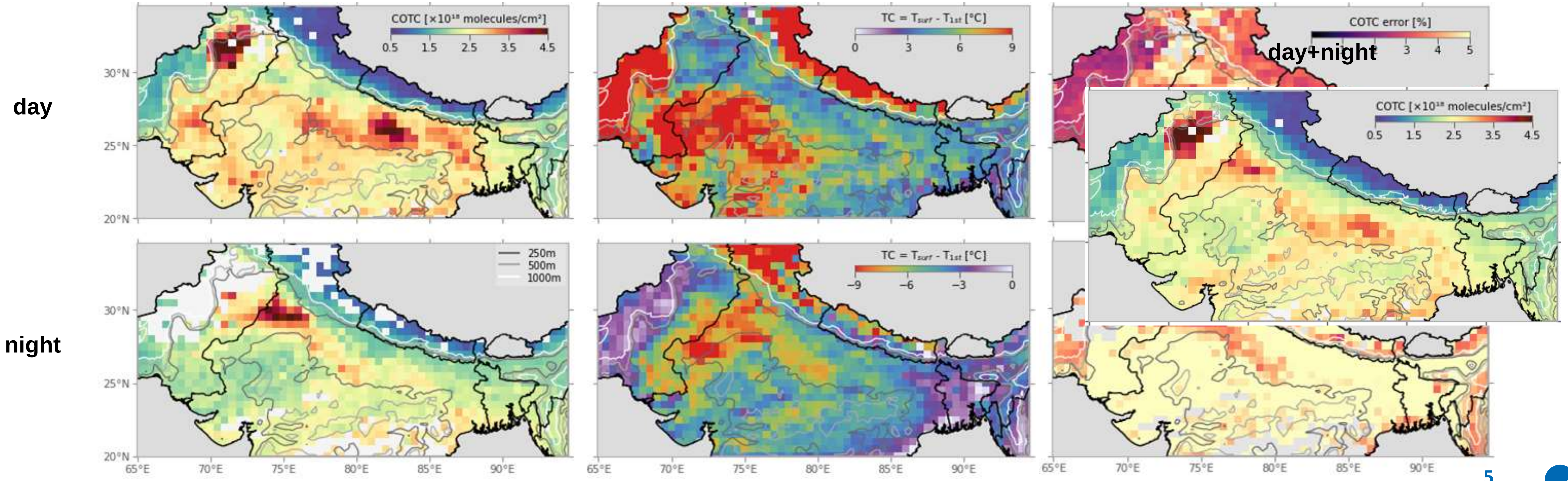

Methods – Combining daytime and nighttime IASI data

- This filter consists of discarding all the IASI pixels for which the error is greater than a certain **threshold**.
- We set the threshold value by comparing IASI with TROPOMI, as it is more sensitive to the surface under clear-sky conditions [Borsdorff et al. 2018].

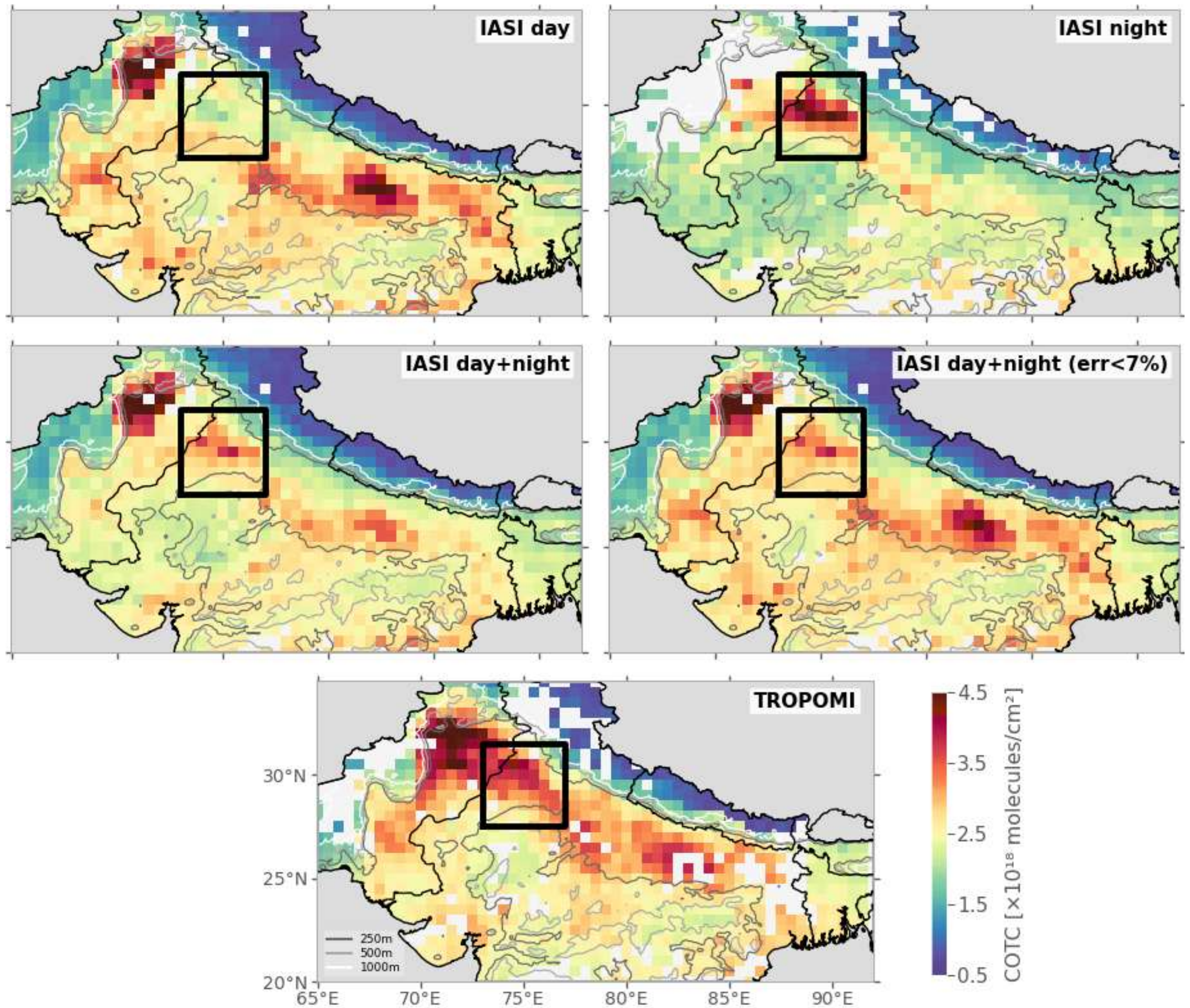

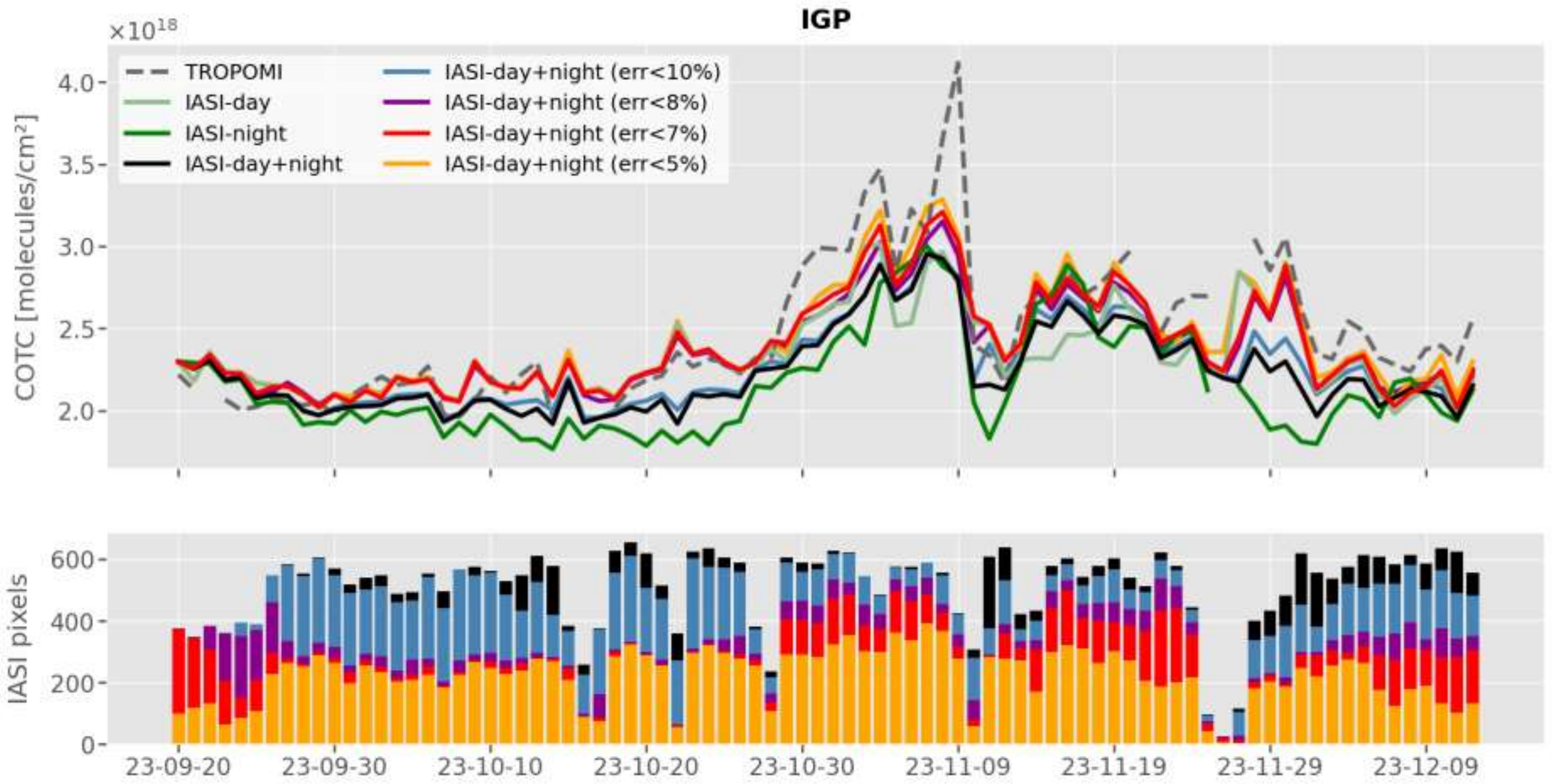

- The lower the threshold, the higher the IASI COTC concentration.

  → **we choose 7% as the threshold value**

IASI CO total column daily evolution from 2007 to 2024, IGP

- Highest CO concentrations are found during the pre-monsoon and the post-monsoon seasons, due to **agricultural waste burning**, as shown by the CO emissions from the Global Fire Emissions Database (GFED4.1s, [van der Werf et al. 2017]).
- Air pollution episodes during the post-monsoon season are highly dependent on **local meteorology**.

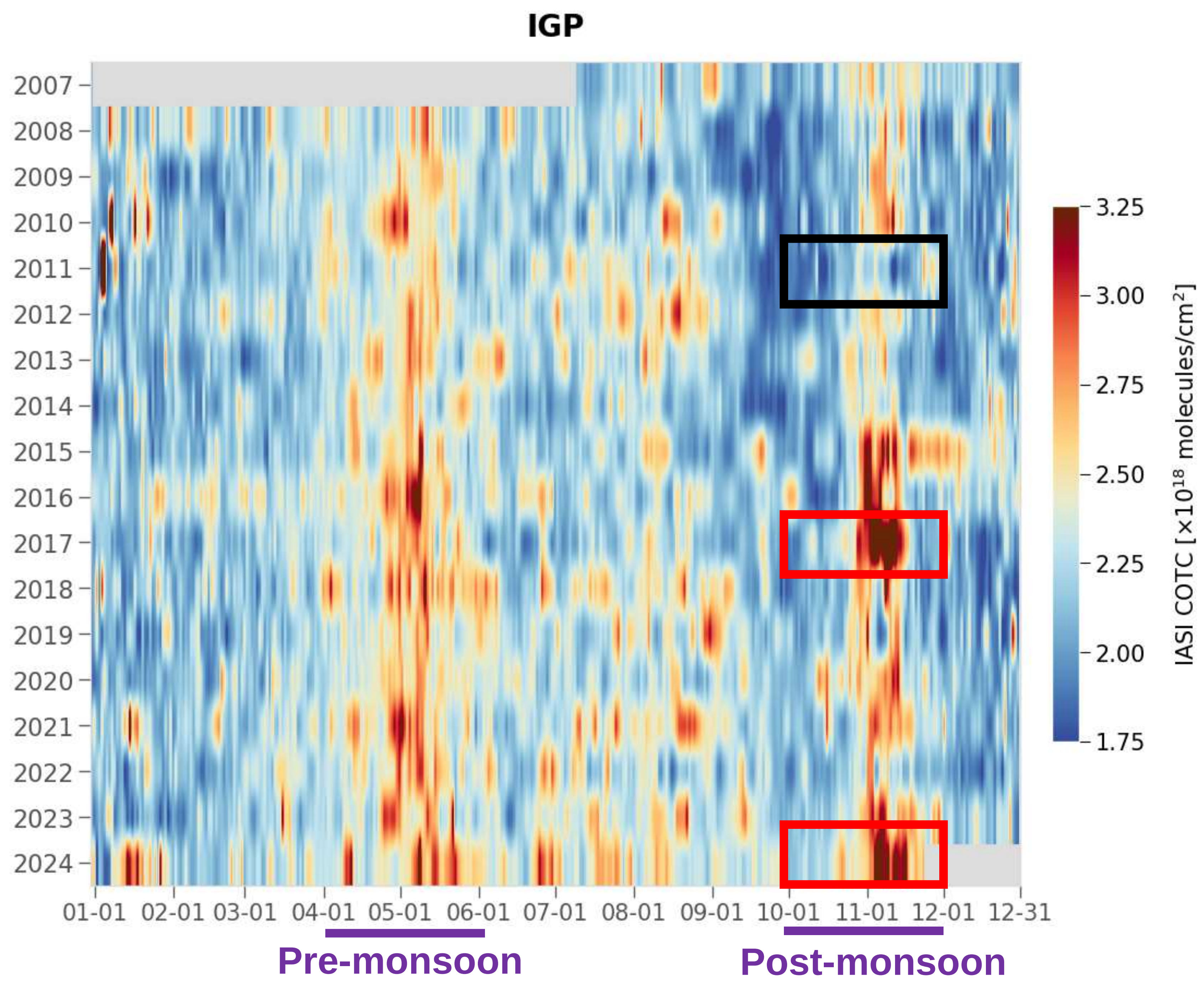

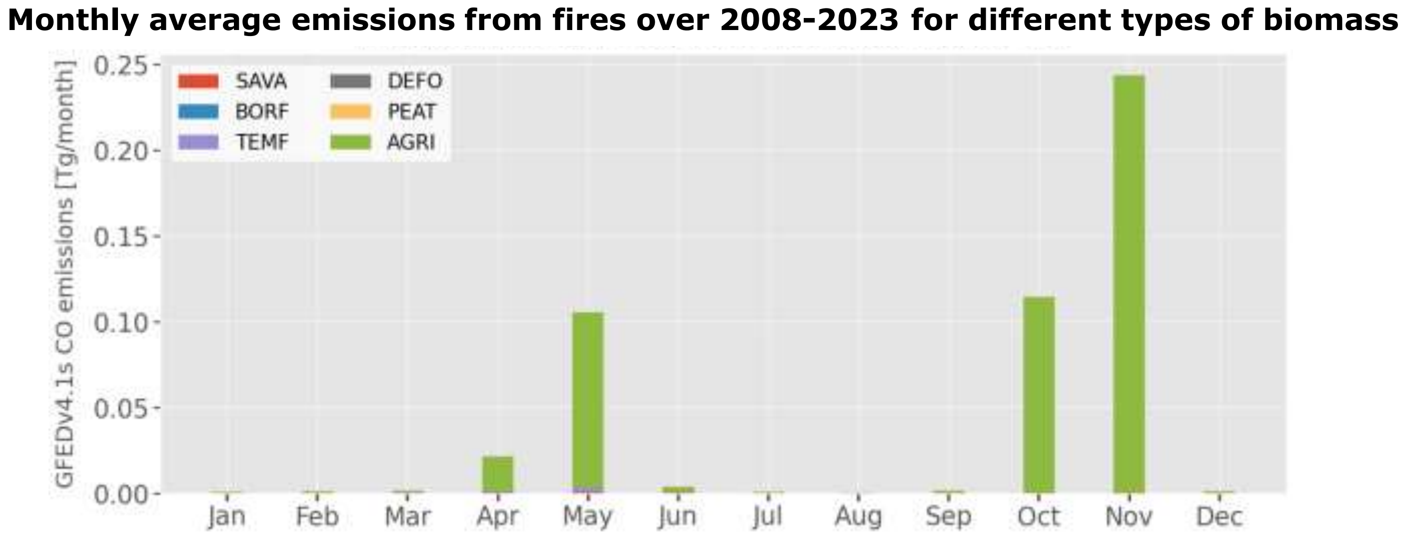

[Sinnathamby et al., 2025, in prep.]

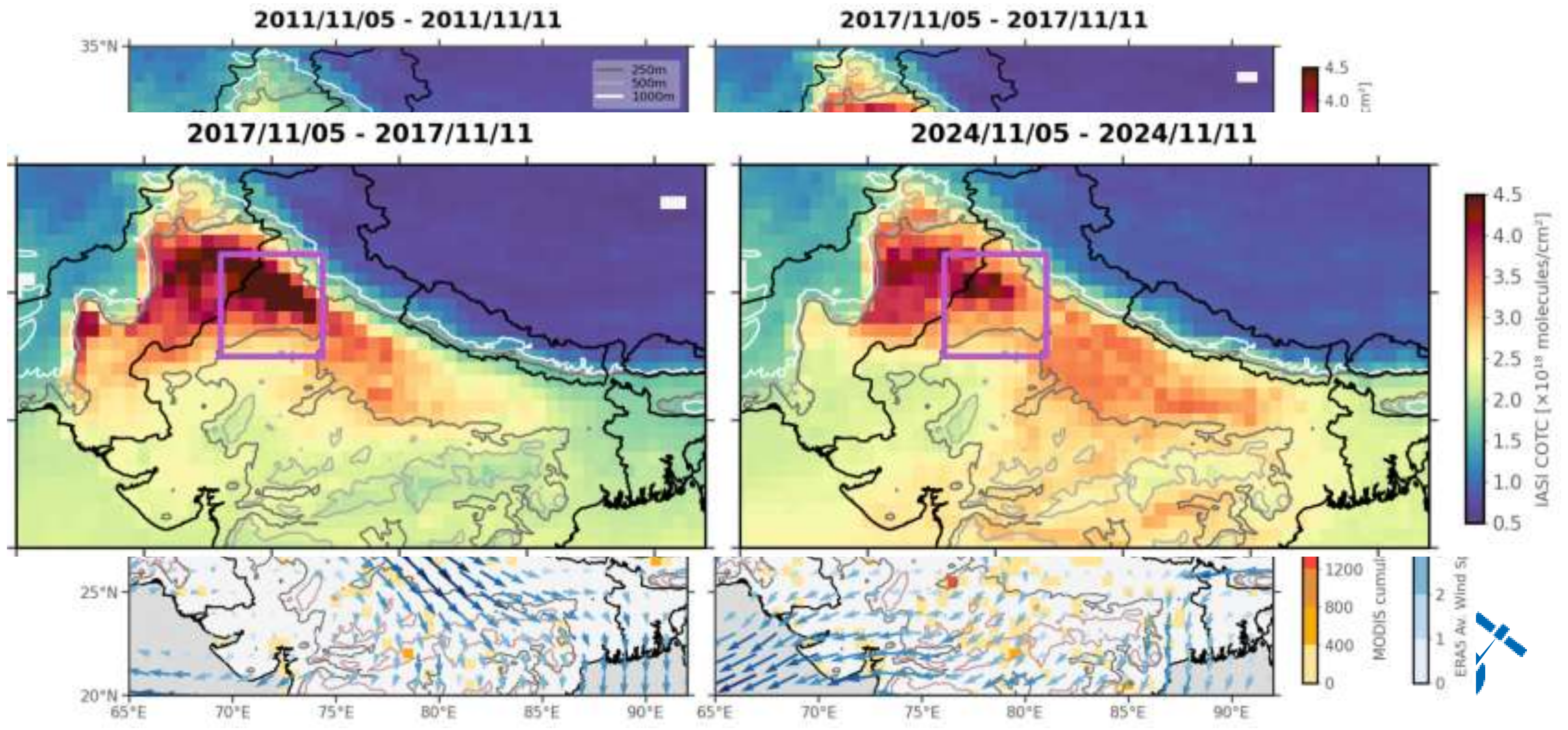

IASI CO total column daily evolution from 2007 to 2024, Mainland SEA

- CO concentrations are the highest during the dry season due to **vegetation fires and agricultural waste burning.**
- CO from Indonesian fires occurring in September are also detected in Mainland SEA.

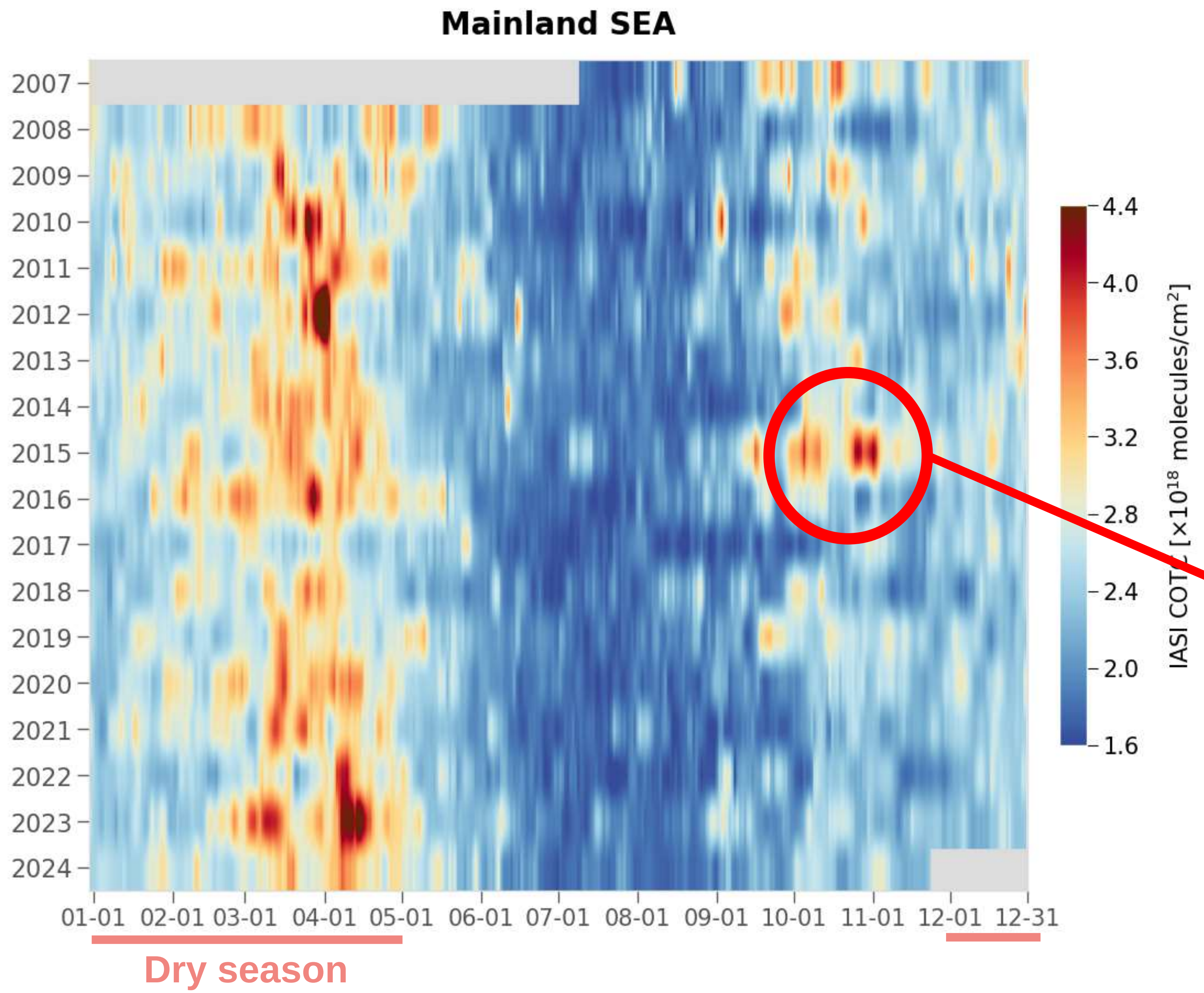

Monthly average emissions from fires over 2008-2023 for different types of biomass

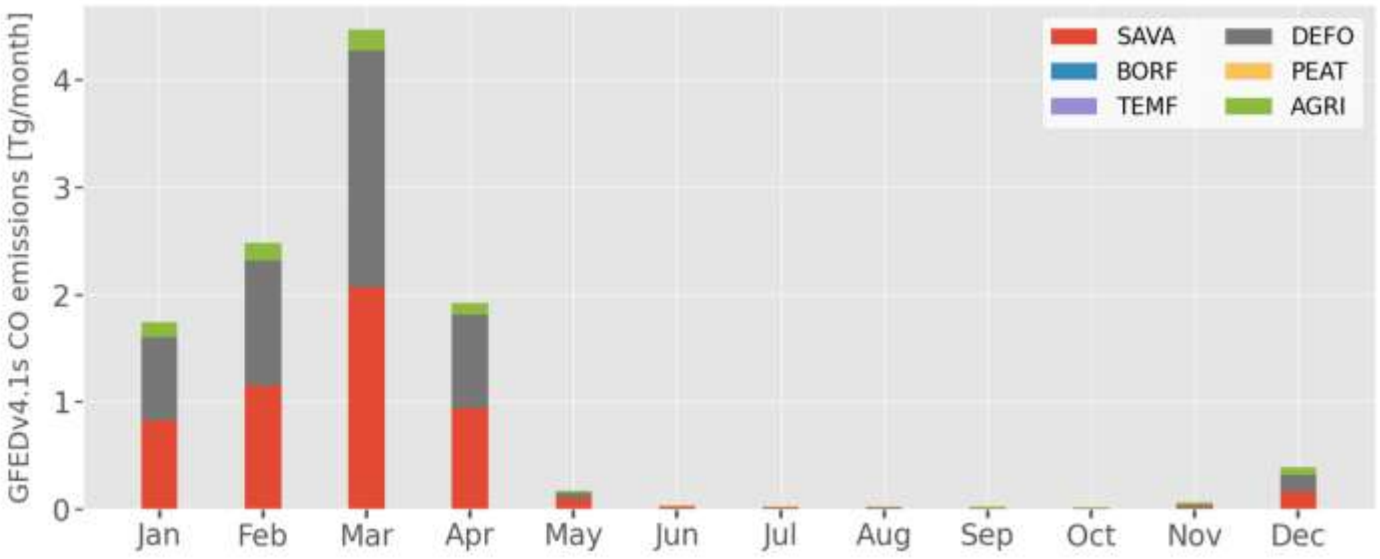

2015/10/25 - 2015/10/30

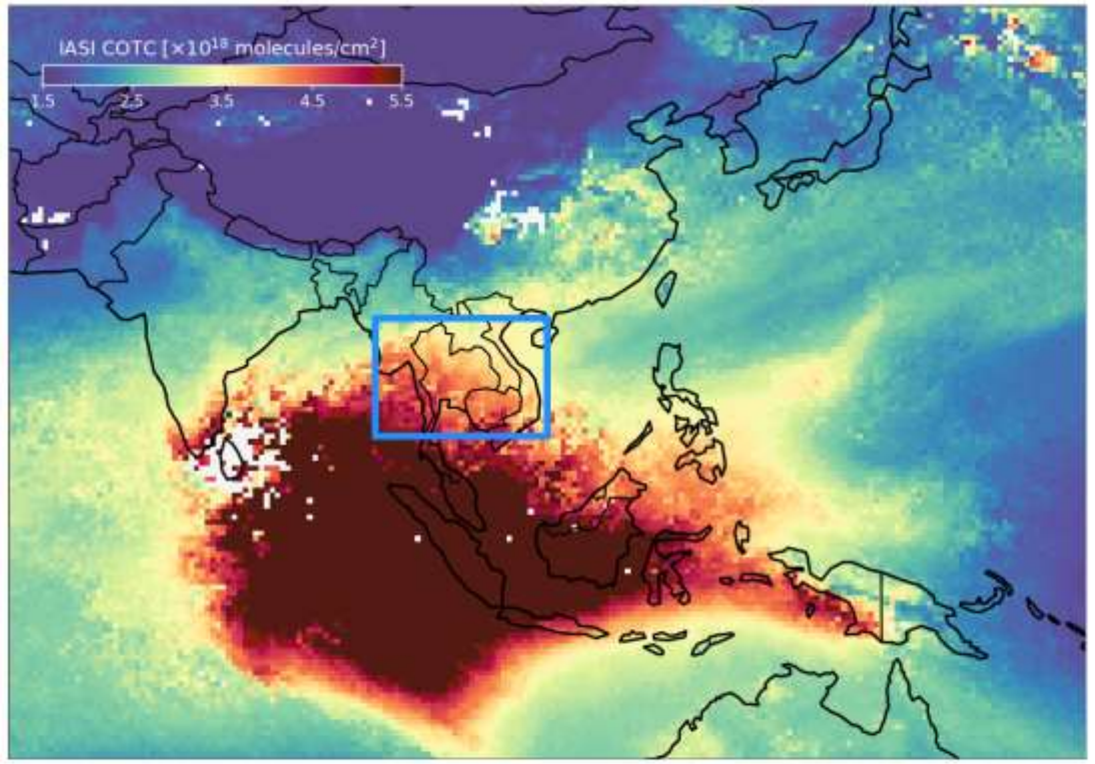

IASI CO total column daily evolution from 2007 to 2024, NCP

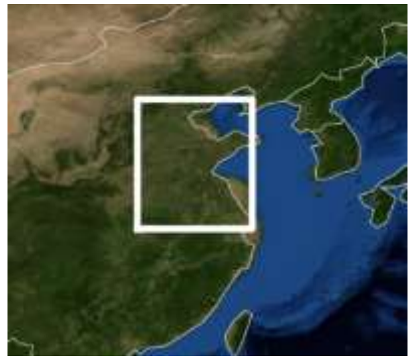

- CO concentrations are the highest during winter and spring, mainly due to **high anthropogenic emissions**, **low OH levels** and **local meteorology** [Boynard et al., 2013].
- In spring, **agricultural waste burning** can contribute to the already elevated CO levels in the region.

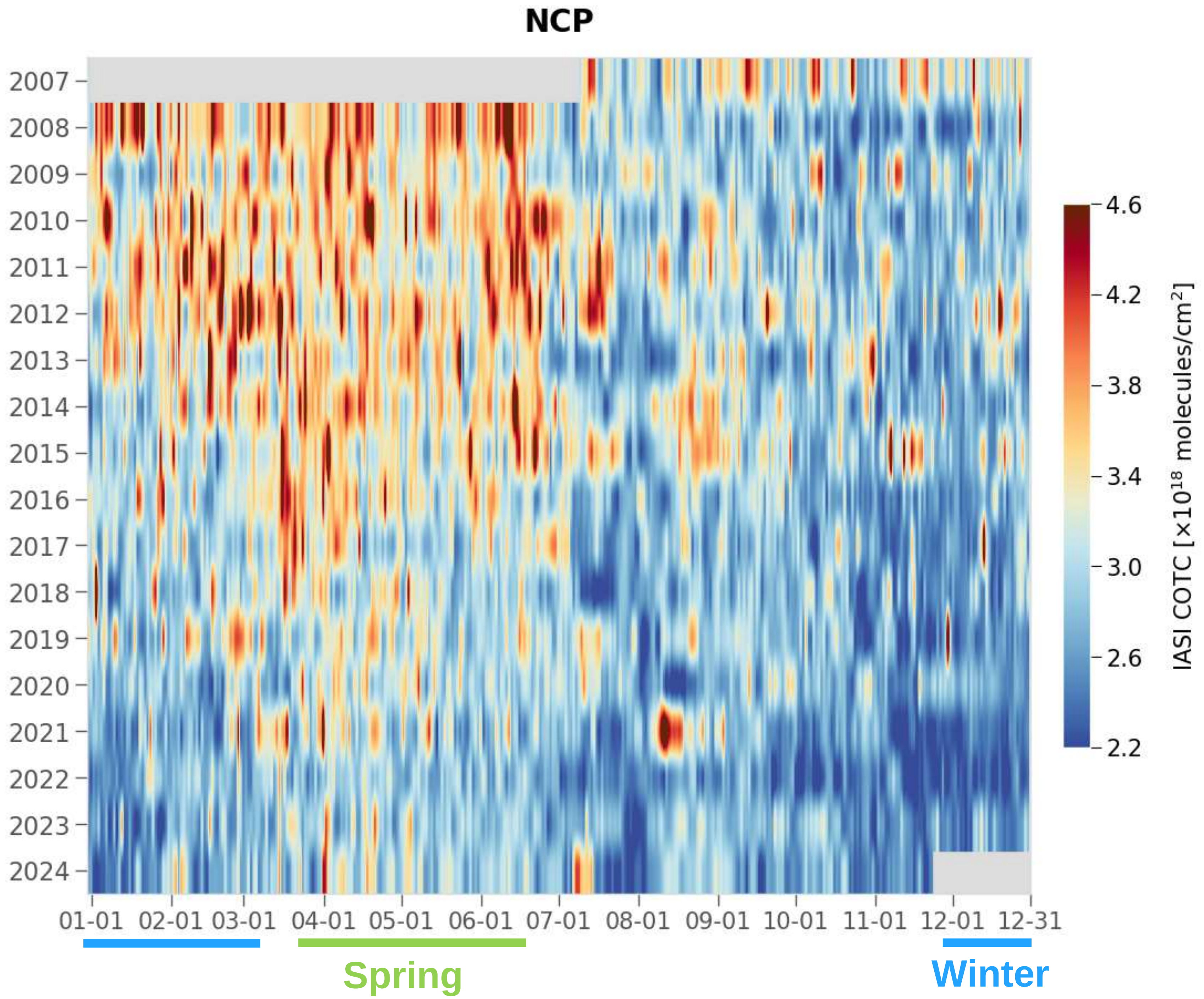

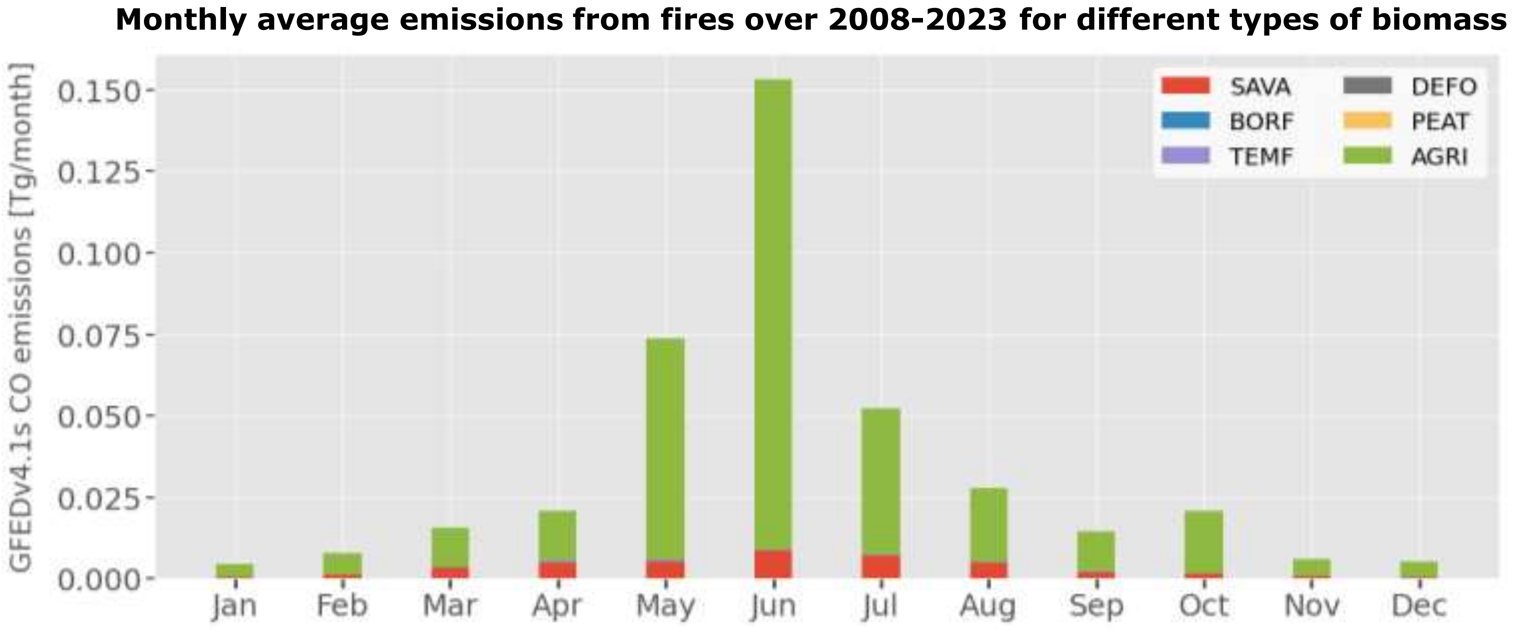

IASI CO total column global trends in Asia [2007/07 – 2024/06]

- Trends are estimated using the **Theil-Sen method (TS)** [Theil, 1950; Sen, 1968] on annual averages of COTC over the period 2007/07-2024/06. Significant trends (p-value < 0.05) are stippled.

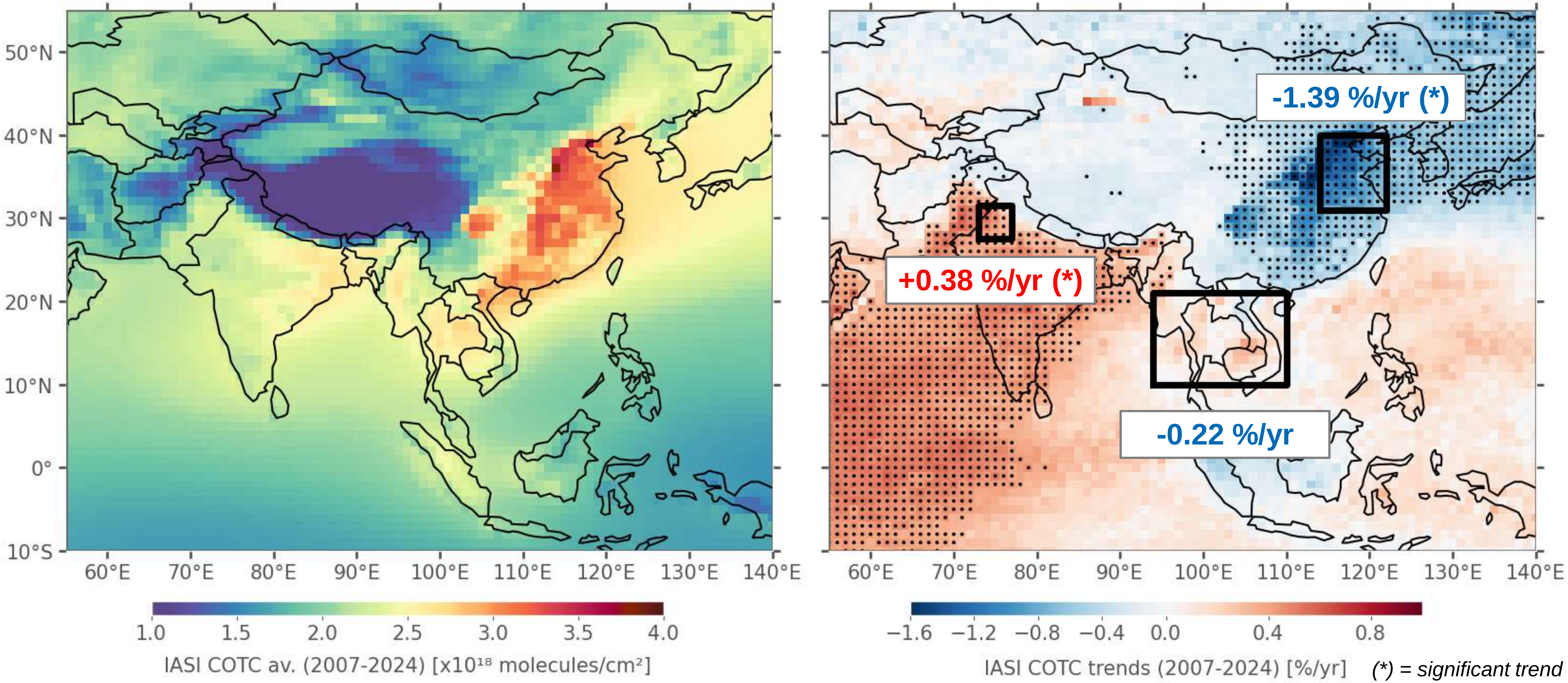

(*) = significant trend

IASI CO total column trends during pollution seasons

- IASI 17-year COTC trends for selected pollution seasons in each region are shown below. Significant trends are marked by an asterix (*).

Winter
(Dec+Jan+Feb+Mar)

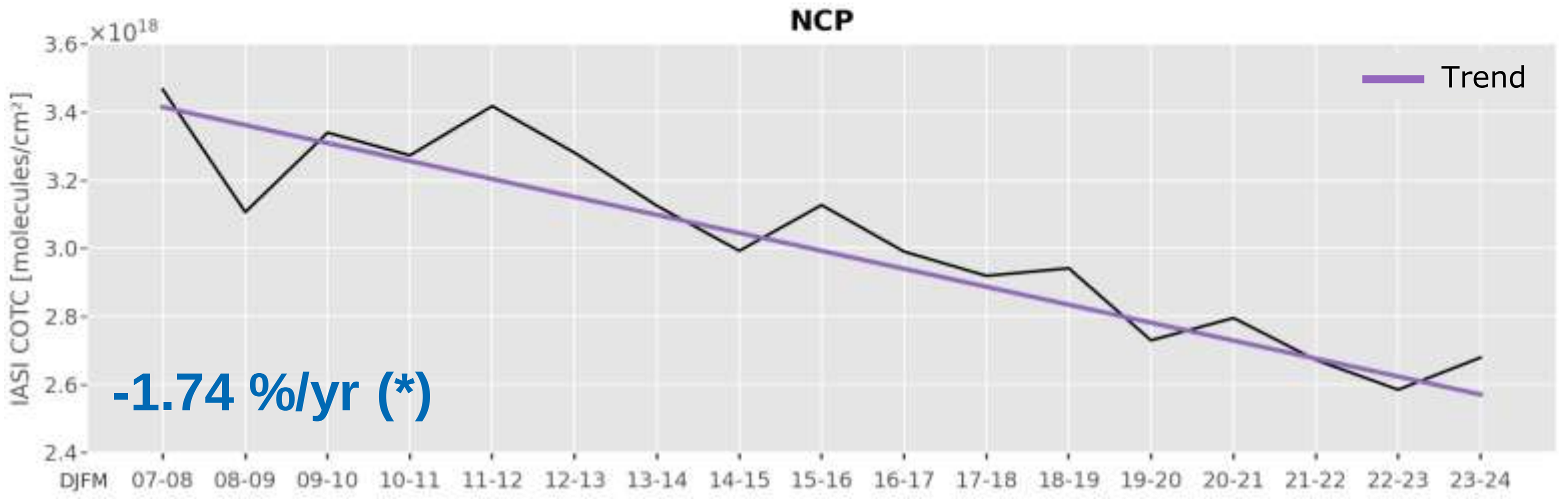

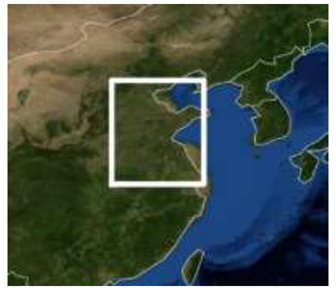

Post-monsoon
(Oct+Nov)

Dry season
(Dec+Jan+Feb+Mar+Apr)

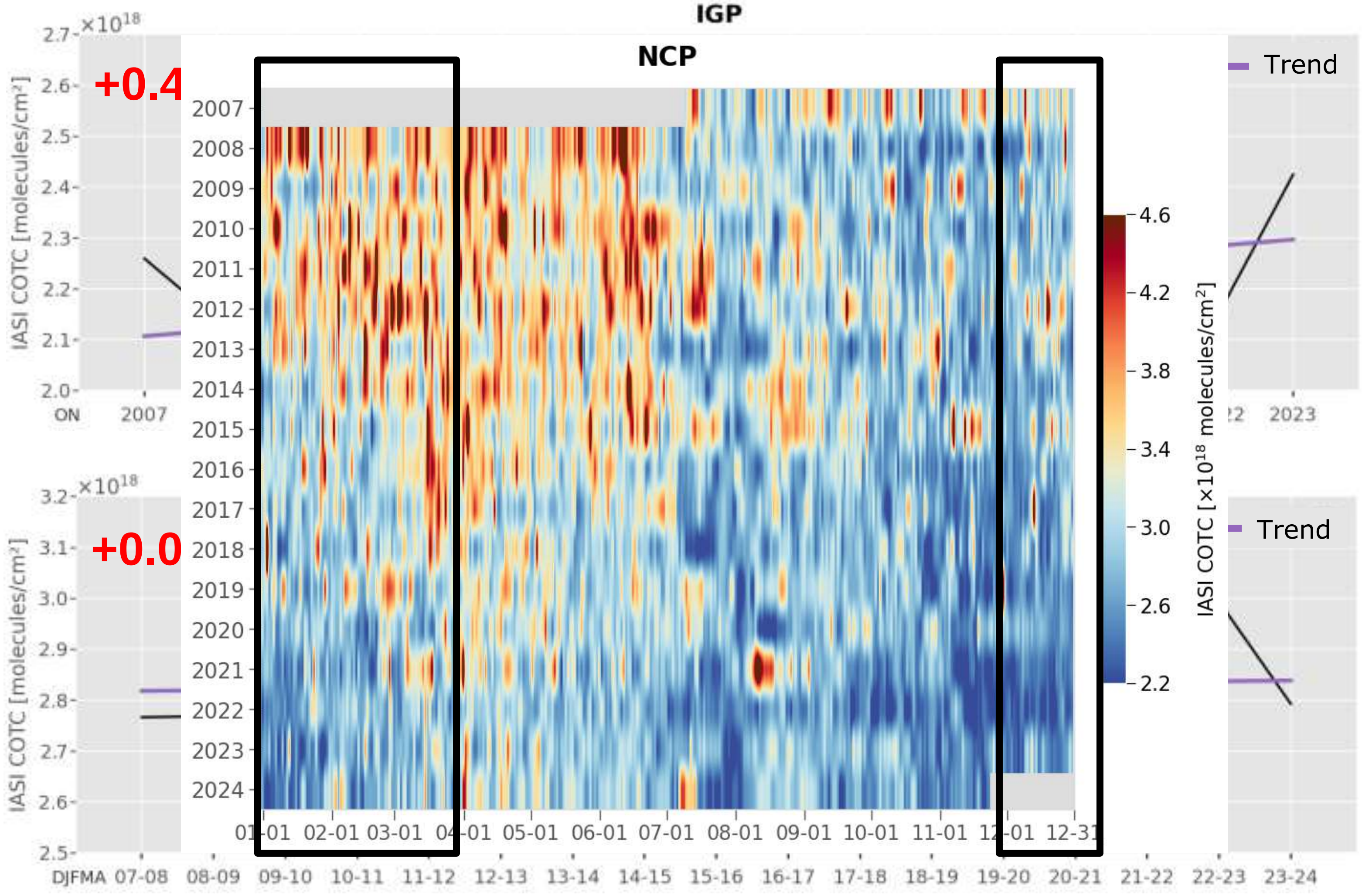

Explaining IASI trends with emission trends

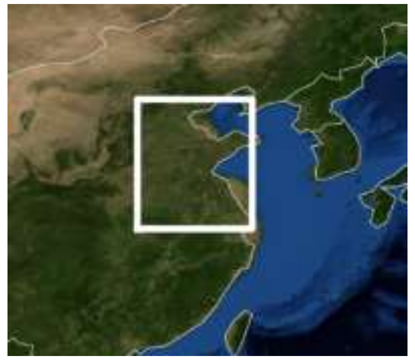

- CO IASI trends are compared to local CO emission trends from anthropogenic activities and biomass burning, estimated by the Copernicus Atmosphere Monitoring Service (CAMS) global anthropogenic emission inventory (**CAMS-GLOB-ANTv6.2**, [Granier et al., 2019]) and Global Fire Assimilation System inventory (**GFASv1.2**, [Kaiser et al., 2012]), respectively.

- During the **winter season in NCP**, the deployment of the **China Air Quality Action Plan** has led to a reduction of CO emissions and as such a coincident decrease in CO concentration.

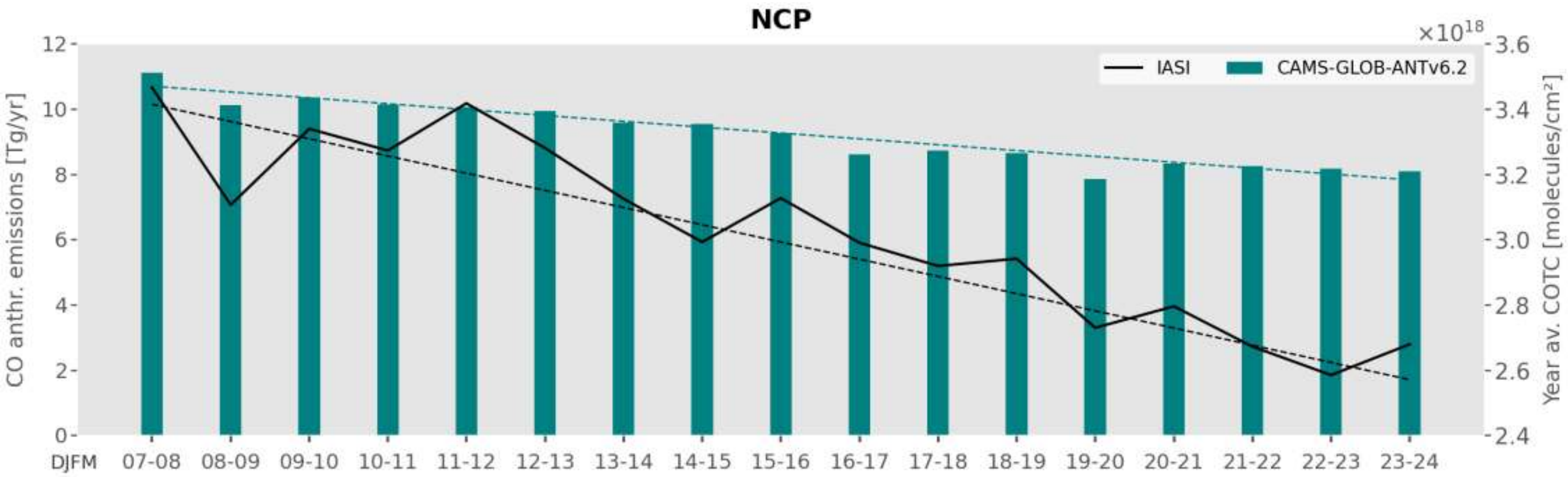

-1.74 %/yr

-179.5 Gg/yr²

Explaining IASI trends with emissions trends

- CO IASI trends are compared to local CO emission trends from anthropogenic activities and biomass burning, estimated by the Copernicus Atmosphere Monitoring Service (CAMS) global anthropogenic emission inventory (**CAMS-GLOB-ANTv6.2**, [Granier et al., 2019]) and Global Fire Assimilation System inventory (**GFASv1.2**, [Kaiser et al., 2012]), respectively.

- For the **post-monsoon season in IGP**, IASI and CAMS show a positive trend, while GFAS shows a negative one, making it hard to explain concentrations trend with emission trends.

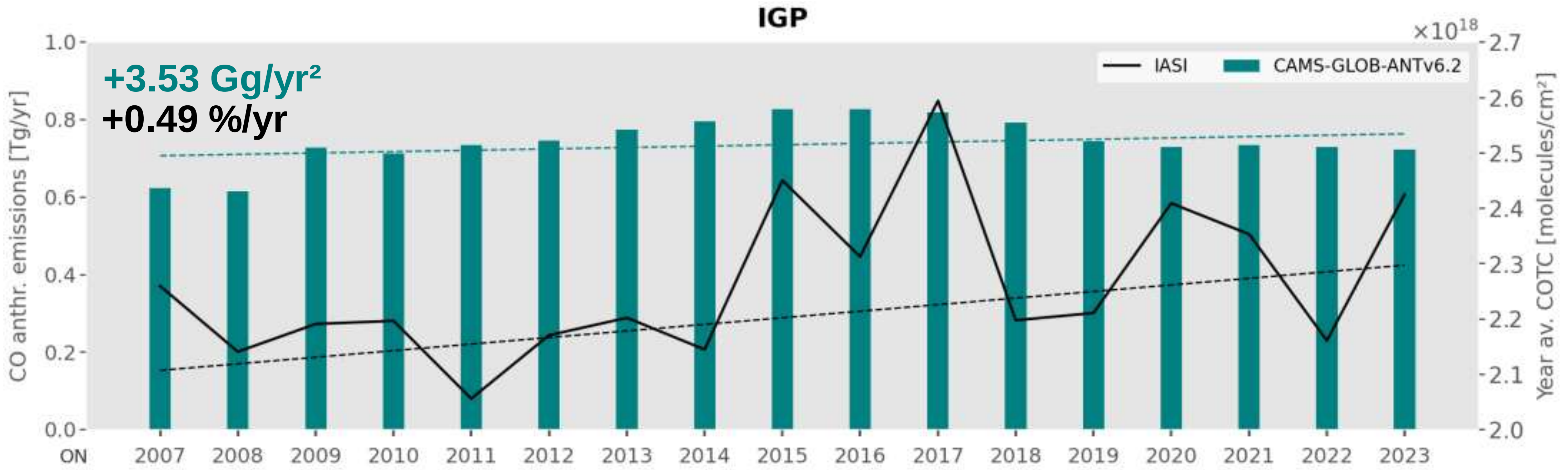

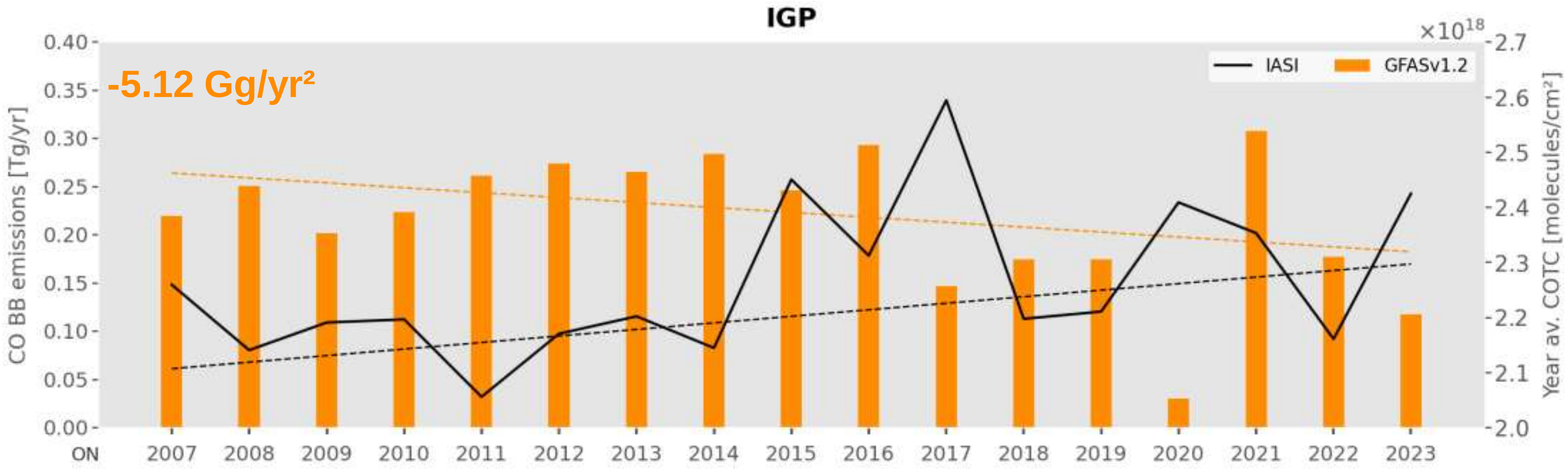

Conclusions and take home messages

- The new reprocessed IASI CO Climate Data Record allows us to conduct trend studies for the first time in heavily polluted regions in Asia.
- We show that nighttime data, usually discarded because of their supposed low sensitivity to the lower atmosphere, can be invaluable for detecting near-surface CO.
- We developed a user-friendly method to only consider IASI pixels that are sensitive to the surface, and so improved the CO surface detection.
- In some regions, CO concentration trends from IASI can be explained by the trends as observed by local emissions inventories.

- **However, relating concentration trends with emission trends remains a challenging exercise, particularly when these ones are built on limited information. Moreover, CO concentrations also depend on transport phenomena, chemical processes and local meteorology, which need to be accounted for in the discussion of the results.**

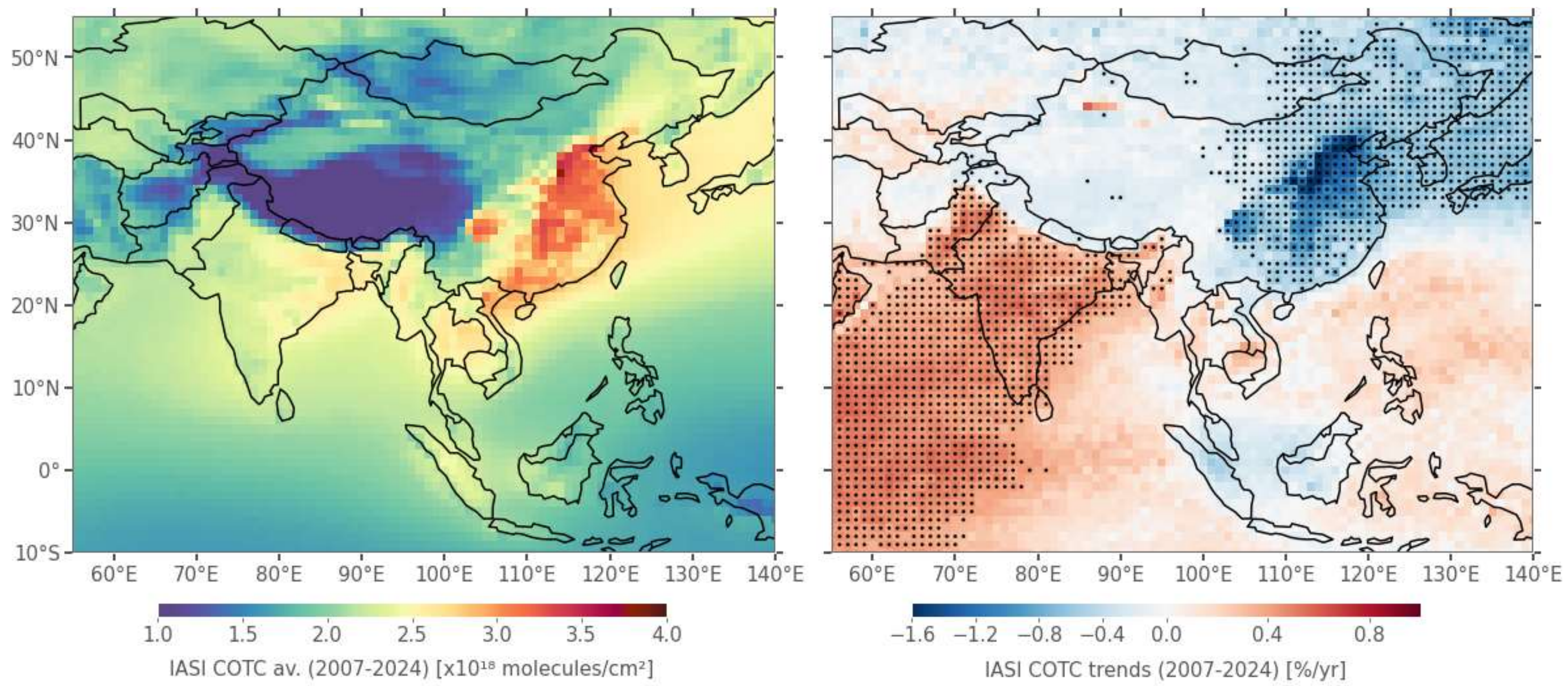

References

- Clerbaux, C., Boynard, A., Clarisse, L., George, M., Hadji-Lazaro, J., Herbin, H., Hurtmans, D., Pommier, M., Razavi, A., Turquety, S., Wespes, C., & Coheur, P. (2009). Monitoring of atmospheric composition using the thermal infrared IASI/MetOp sounder. Atmospheric Chemistry and Physics, 9(16), 6041–6054. https://doi.org/10.5194/acp-9-6041-2009
- Holloway, T., Levy, H., & Kasibhatla, P. (2000). Global distribution of carbon monoxide. Journal of Geophysical Research Atmospheres, 105(D10), 12123–12147. https://doi.org/10.1029/1999jd901173
- George, M., Clerbaux, C., Bouarar, I., Coheur, P., Deeter, M. N., Edwards, D. P., Francis, G., Gille, J. C., Hadji-Lazaro, J., Hurtmans, D., Inness, A., Mao, D., & Worden, H. M. (2015). An examination of the long-term CO records from MOPITT and IASI: comparison of retrieval methodology. Atmospheric Measurement Techniques, 8(10), 4313–4328. https://doi.org/10.5194/amt-8-4313-2015
- Bauduin, S., Clarisse, L., Theunissen, M., George, M., Hurtmans, D., Clerbaux, C., & Coheur, P. (2017). IASI's sensitivity to near-surface carbon monoxide (CO): Theoretical analyses and retrievals on test cases. Journal of Quantitative Spectroscopy and Radiative Transfer, 189, 428–440. https://doi.org/10.1016/j.jqsrt.2016.12.022
- Borsdorff, T., De Brugh, J. A., Hu, H., Hasekamp, O., Sussmann, R., Rettinger, M., Hase, F., Gross, J., Schneider, M., Garcia, O., Stremme, W., Grutter, M., Feist, D. G., Arnold, S. G., De Mazière, M., Sha, M. K., Pollard, D. F., Kiel, M., Roehl, C., . . . Landgraf, J. (2018). Mapping carbon monoxide pollution from space down to city scales with daily global coverage. Atmospheric Measurement Techniques, 11(10), 5507–5518. https://doi.org/10.5194/amt-11-5507-2018
- Boynard, A., Clerbaux, C., Clarisse, L., Safieddine, S., Pommier, M., Van Damme, M., Bauduin, S., Oudot, C., Hadji-Lazaro, J., Hurtmans, D., & Coheur, P. (2014). First simultaneous space measurements of atmospheric pollutants in the boundary layer from IASI: A case study in the North China Plain. Geophysical Research Letters, 41(2), 645–651. https://doi.org/10.1002/2013gl058333
- Van Der Werf, G. R., Randerson, J. T., Giglio, L., Van Leeuwen, T. T., Chen, Y., Rogers, B. M., Mu, M., Van Marle, M. J. E., Morton, D. C., Collatz, G. J., Yokelson, R. J., & Kasibhatla, P. S. (2017). Global fire emissions estimates during 1997–2016. Earth System Science Data, 9(2), 697–720. https://doi.org/10.5194/essd-9-697-2017
- Theil, H. (1950). A rank-invariant method of linear and polynomial regression analysis, 3; confidence regions for the parameters of polynomial regression equations. Indagationes Mathematicae, 1(2), 467–482. https://ir.cwi.nl/pub/18448/18448A.pdf
- Sen, P. K. (1968). Estimates of the regression coefficient based on Kendall's TAU. Journal of the American Statistical Association, 63(324), 1379–1389. https://doi.org/10.1080/01621459.1968.10480934
- Granier, C., Darras, S., Van Der Gon, H. D., Jana, D., Elguindi, N., Bo, G., Michael, G., Marc, G., Jalkanen, J., Kuenen, J., Liousse, C., Quack, B., Simpson, D., & Sindelarova, K. (2019). The Copernicus Atmosphere Monitoring Service global and regional emissions (April 2019 version). HAL (Le Centre Pour La Communication Scientifique Directe). https://doi.org/10.24380/d0bn-kx16
- Kaiser, J. W., Heil, A., Andreae, M. O., Benedetti, A., Chubarova, N., Jones, L., Morcrette, J., Razinger, M., Schultz, M. G., Suttie, M., & Van Der Werf, G. R. (2012). Biomass burning emissions estimated with a global fire assimilation system based on observed fire radiative power. Biogeosciences, 9(1), 527–554. https://doi.org/10.5194/bg-9-527-2012

Back-up - IASI COTC vs CO 0-2km

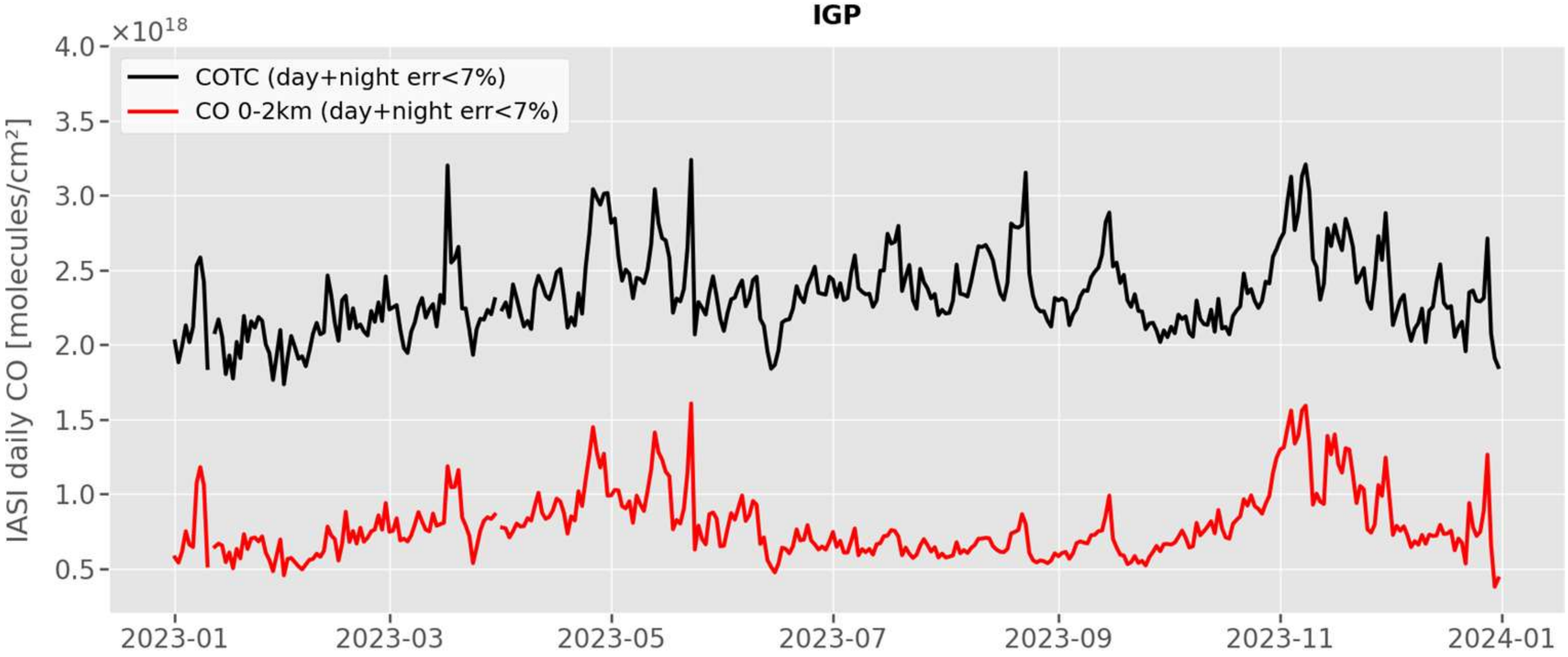

Back-up – GFAS vs GFED

- Annual timeseries of CO fire emissions from GFASv1.2 and GFED4.1s and COTC concentrations from IASI.

-3.3 Gg/yr²
-8.6 Gg/yr²
+0.4 %/yr

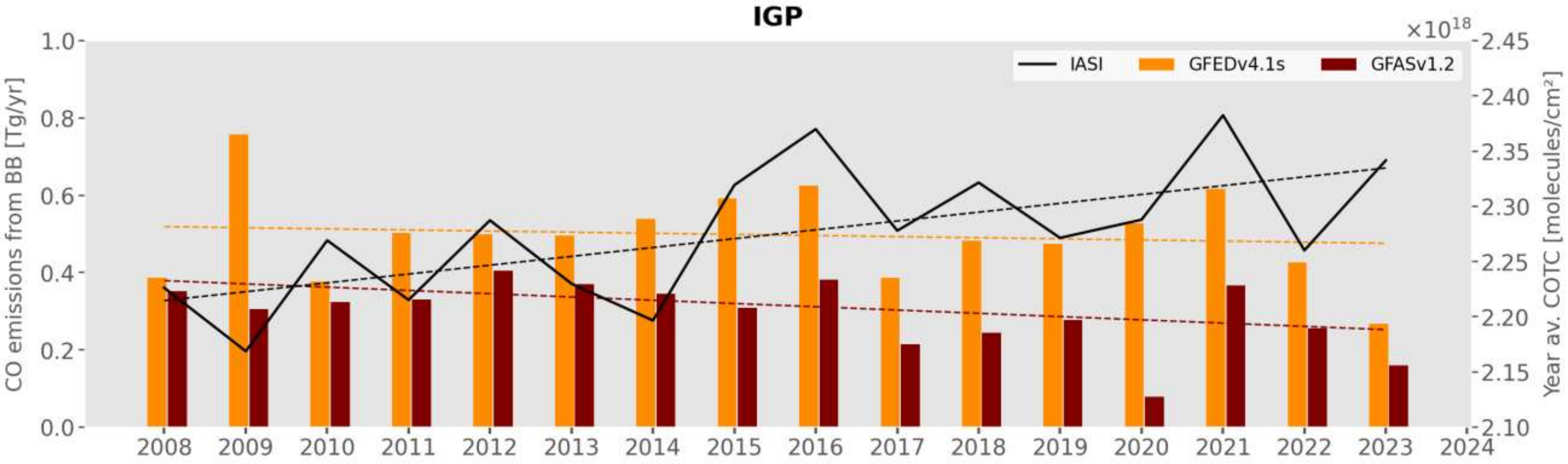

Back-up - IASI trends with WLS method

- The **Weighted Least Squares** (**WLS**) method is a linear regression that is robust to outliers. Trend magnitudes are estimated from the monthly CO anomalies time series. We defined the monthly variance of CO concentrations as weights. Significant trends to 1 standard-error are stippled. The standard error for the WLS method is also given.

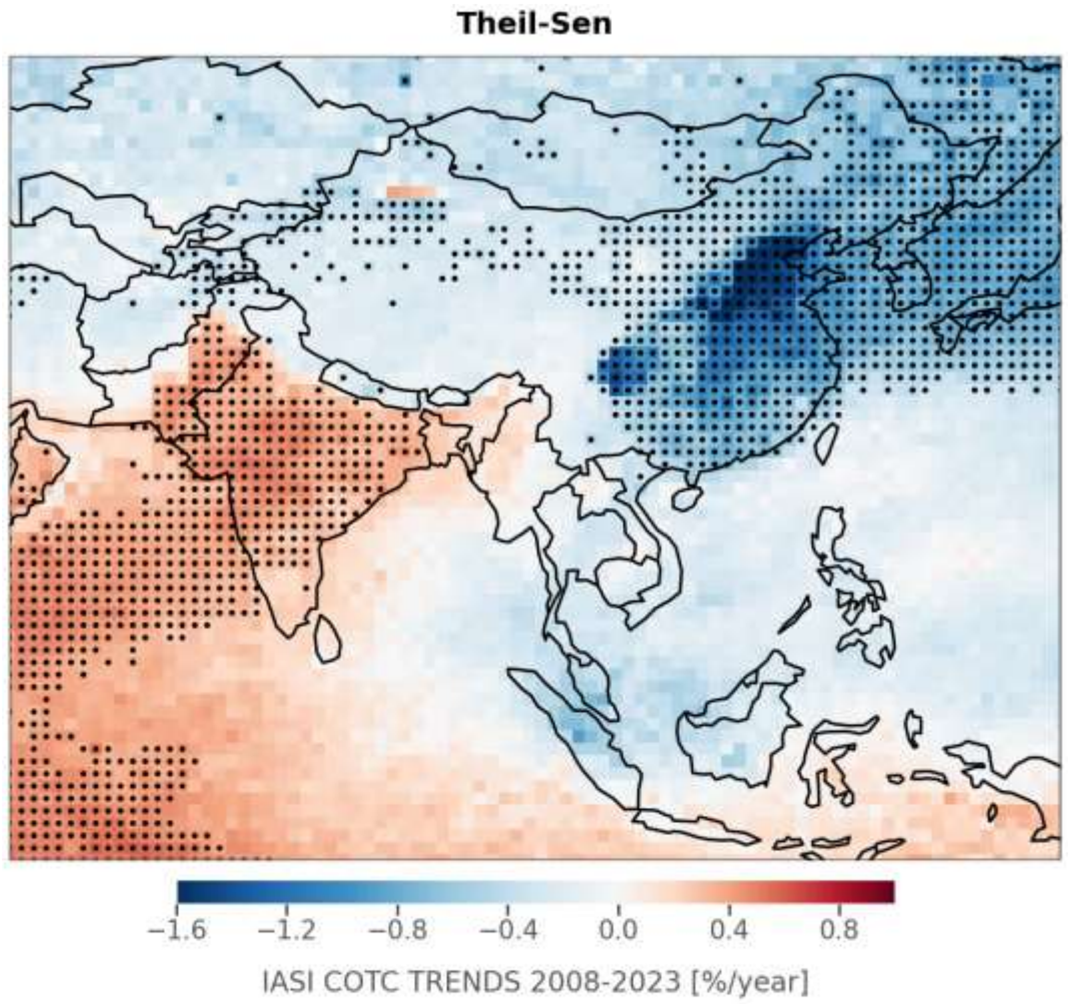

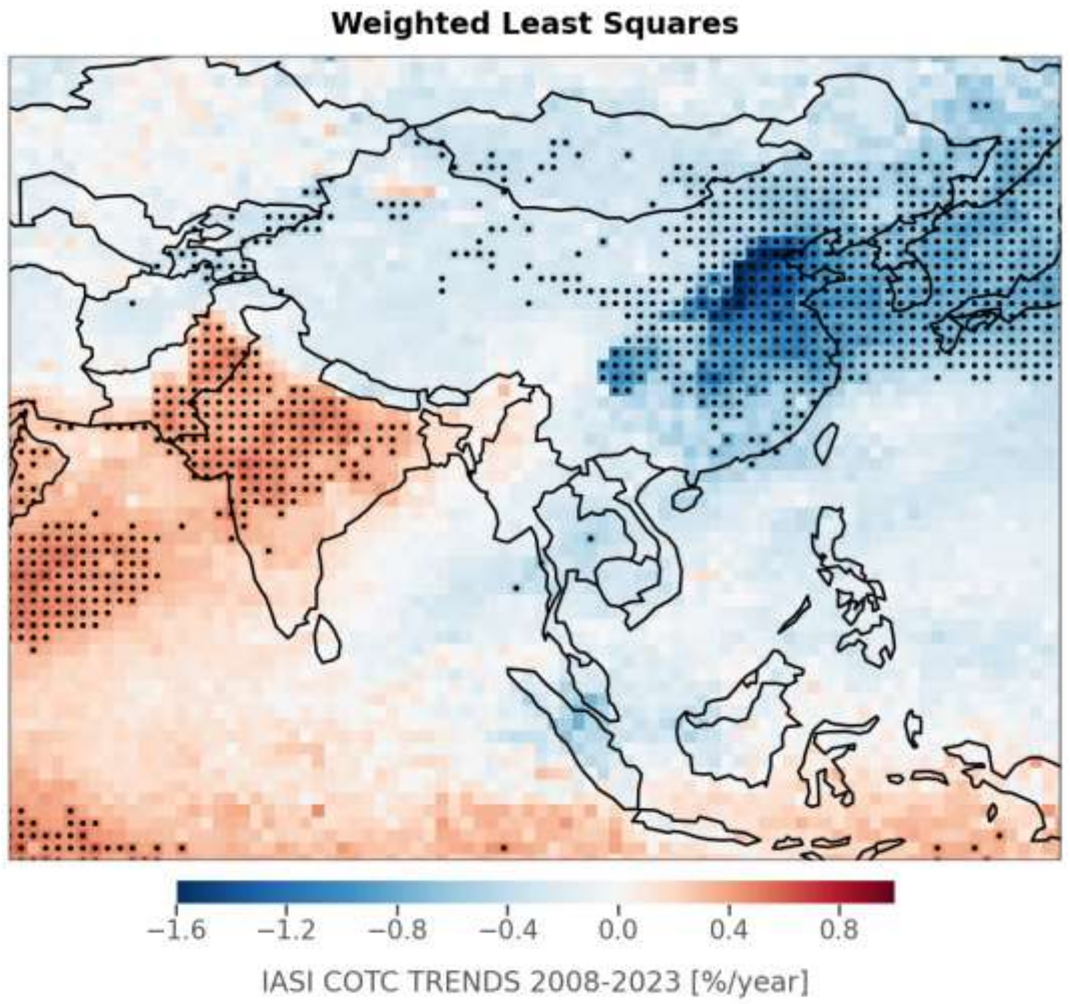

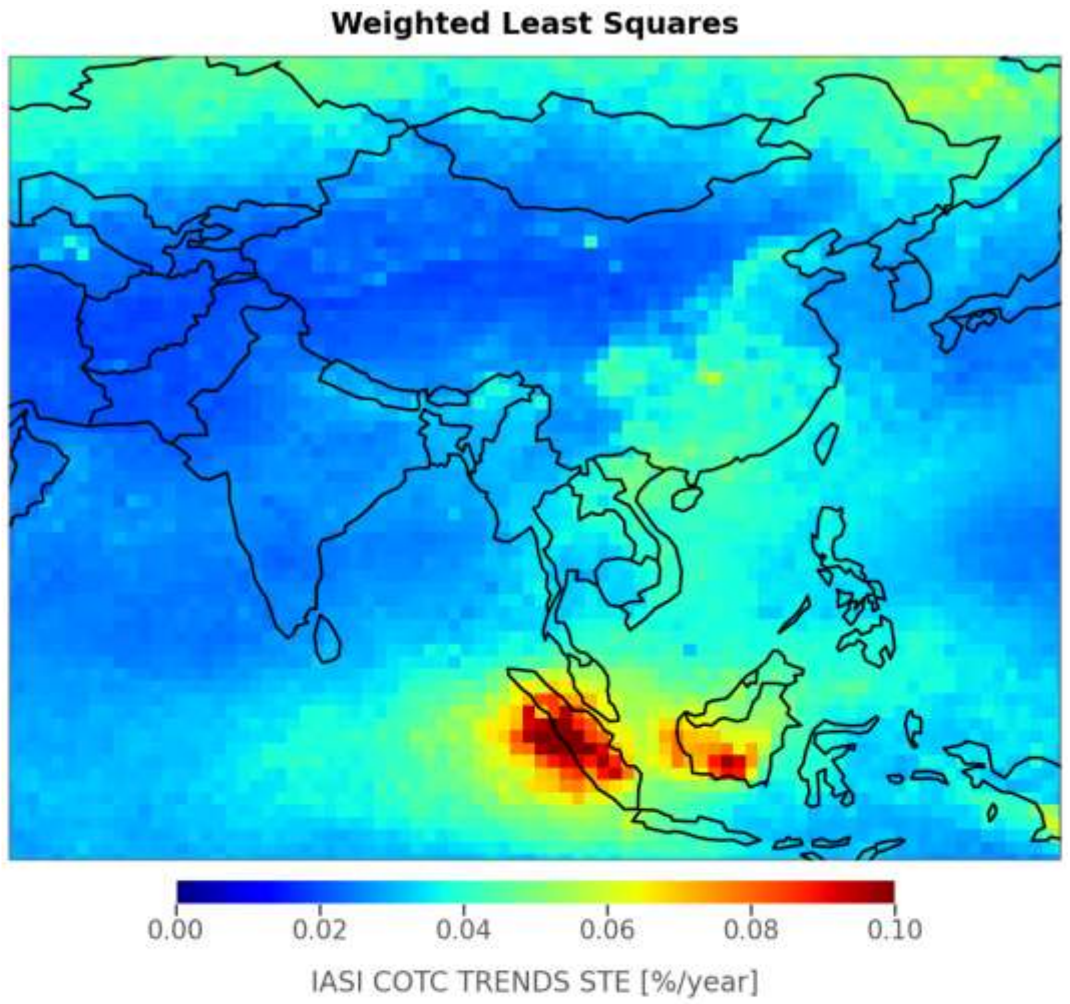

Back-up - Explaining IASI trends with emission in Mainland SEA (dry season)

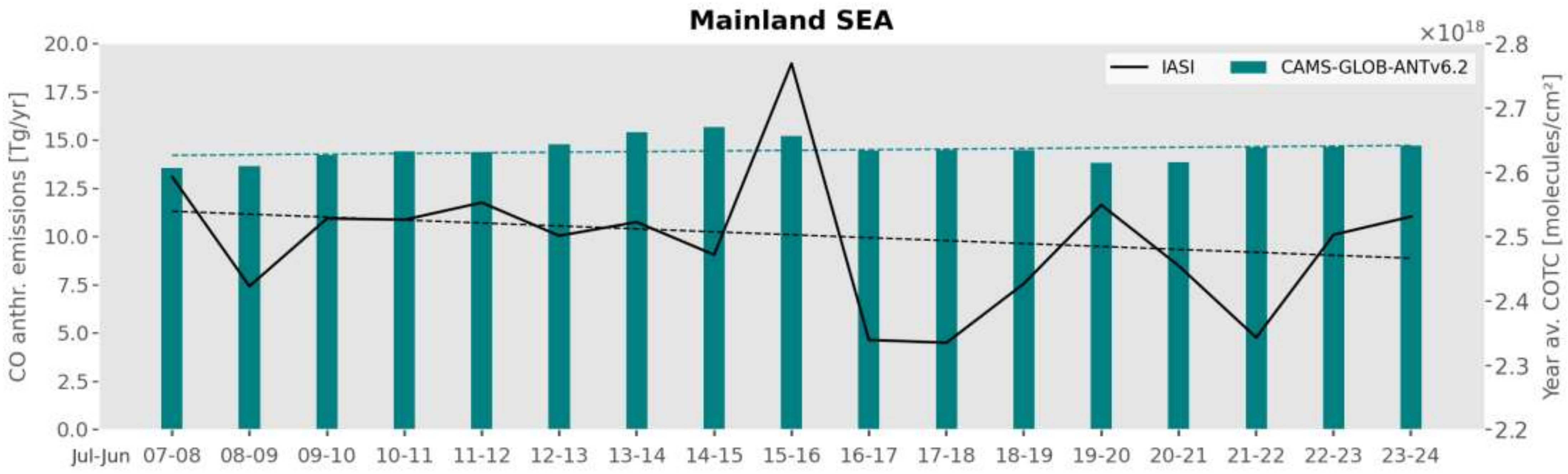

+30.2 Gg/yr²

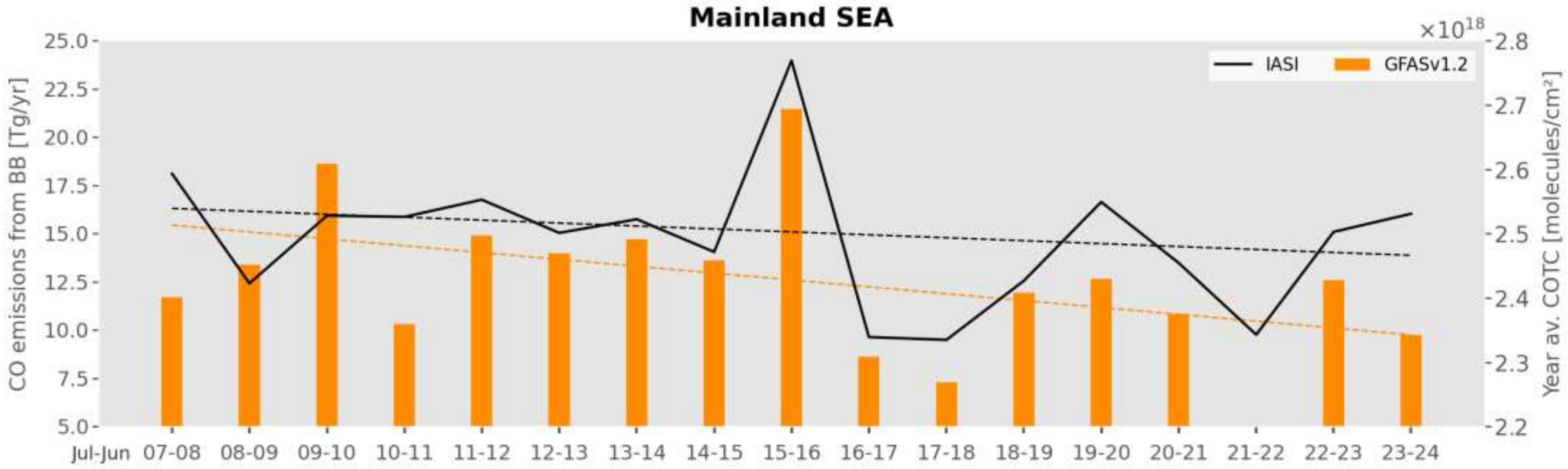

-361.2 Gg/yr²

-0.20 %/yr